

Immunotherapeutic Significance of a Prognostic Alternative Splicing Signature in Bladder Cancer

Technology in Cancer Research & Treatment
Volume 21: 1-13
© The Author(s) 2022
Article reuse guidelines:
sagepub.com/journals-permissions
DOI: [10.1177/15330338221090093](https://doi.org/10.1177/15330338221090093)
journals.sagepub.com/home/tct


Jiang Chen, MD^{1,*} , Yangjie Liao, MD^{2,*} , Rui Li, MD^{3,4,*}, Mingjiang Luo, MD¹ , Guanlin Wu, MD⁵, Ruirong Tan, PhD^{3,6} , and Zhihong Xiao, MD¹

Abstract

Objectives: Bladder cancer is the fourth most common malignancy in men in the United States. Aberrant alternative splicing (AS) events are involved in the carcinogenesis, but the association between AS and bladder cancer remains unclear. This study aimed to construct an AS-based prognostic signature and elucidate the role of the tumor immune microenvironment (TIME) and the response to immunotherapy and chemotherapy in bladder cancer. **Methods:** Univariate Cox regression analysis was performed to detect prognosis-related AS events. The least absolute shrinkage and selection operator (LASSO) and multivariate Cox analyses were employed to build prognostic signatures. Kaplan–Meier survival analysis, multivariate Cox regression analysis, and receiver operating characteristic (ROC) curves were conducted to validate the prognostic signatures. Then, the Estimation of Stromal and Immune cells in MAlignant Tumor tissues using Expression data (ESTIMATE) and tumor immune estimation resource (TIMER) databases were searched and the single-sample gene set enrichment analysis (ssGSEA) algorithm and CIBERSORT method were performed to uncover the context of TIME in bladder cancer. The Tumor Immune Dysfunction and Exclusion (TIDE) web tool and pRRophetic algorithm were used to predict the response to immunotherapy and chemotherapy. Finally, we constructed a correlation network between splicing factors (SFs) and survival-related AS events. **Results:** A total of 4684 AS events were significantly associated with overall survival in patients with bladder cancer. Eight prognostic signatures of bladder cancer were established, and a clinical survival prediction model was built. In addition, the consolidated prognostic signature was closely related to immune infiltration and the response to immunotherapy and chemotherapy. Furthermore, the correlation identified EIF3A, DDX21, SDE2, TNPO1, and RNF40 as hub SFs, and function analysis found ubiquitin-mediated proteolysis is correlated most significantly with survival-associated AS events. **Conclusion:** Our findings highlight the prognostic value of AS for patients with bladder cancer and reveal pivotal players of AS events in the context of TIME and the response to immunotherapy and chemotherapy, which may be important for patient management and treatment.

Keywords

Bladder cancer, alternative splicing, prognostic, tumor immune microenvironment, immunotherapeutic, drug response

¹ The Second Affiliated Hospital, Hengyang Medical School, University of South China, Hengyang, China

² The Third Xiangya Hospital of Central South University, Changsha, Hunan, PR China

³ Cedars-Sinai Samuel Oschin Comprehensive Cancer Institute, Los Angeles, CA, USA

⁴ Sichuan Cancer Center, School of Medicine, Sichuan Cancer Hospital and Institute, University of Electronic Science and Technology of China, Chengdu, China

⁵ School of Basic Medical Sciences, Fudan University, Shanghai, China

⁶ International Center for Translational Chinese Medicine, Sichuan Academy of Chinese Medicine Sciences, Chengdu, China

*Jiang Chen, Yangjie Liao, and Rui Li contributed equally to this work.

Corresponding Authors:

Zhihong Xiao, MD, The Second Affiliated Hospital, Hengyang Medical School, University of South China, Hengyang, 421000, China.
Email: x35042875@gmail.com

Ruirong Tan, PhD, Cedars-Sinai Samuel Oschin Comprehensive Cancer Institute, Los Angeles, CA, 90001, USA.
Email: ruirongtan@163.com



Abbreviations

AA, alternate acceptor site; AD, alternate donor site; AP, alternate promoter; AS, alternative splicing; AT, alternate terminator; CI, confidence interval; ES, exon skip; ESTIMATE, Estimation of Stromal and Immune cells in MAlignant Tumor tissues using Expression data; FDR, false-discovery rate; GO, Gene Ontology; HR, hazard ratio; ICIs, immune checkpoint inhibitors; IC50, half maximal inhibitory concentration; KEGG, Kyoto Encyclopedia of Genes and Genomes; LASSO, least absolute shrinkage and selection operator; MDSC, myeloid-derived suppressor cell; ME, mutually exclusive exons; mRNA, messenger RNA; OS, overall survival; PSI, Percent Spliced-In; RI, retained intron; ROC, receiver operating characteristic; SFs, splicing factors; ssGSEA, single-sample gene set enrichment analysis; TCGA, The Cancer Genome Atlas; TCGA-BLCA, The Cancer Genome Atlas Urothelial Bladder Carcinoma; TIME, tumor immune microenvironment; TIMER, tumor immune estimation resource; TIDE, Tumor Immune Dysfunction and Exclusion; Tregs, regulatory T cells; TAM, tumor-associated macrophages.

Received: November 17, 2021; Revised: February 17, 2022; Accepted: February 27, 2022.

Introduction

Bladder cancer is one of the most common malignant tumors of the urinary system, affecting about 430,000 patients and killing about 165,000 patients annually.^{1,2} Despite the fact that the current clinical stages and histopathologic classification for bladder cancer employ widely used prognostic tools, key points with regard to the prediction about recurrence and metastasis of bladder cancer remain unclear.^{3–6} Therefore, it is necessary to explore the molecular mechanisms of bladder cancer occurrence and development to identify novel prognostic biomarkers and potential therapeutic targets.

Previous studies have reported that tumor immunity plays an important role in the occurrence, development, treatment, and treatment resistance of bladder cancer. The transition from a tumor-killing immune microenvironment to an immunosuppressive microenvironment is an important aspect of tumor progression.^{7–9} Immune checkpoints are surface proteins on T cells and other immune cells that act as negative regulators of immune activation through various antigens, including tumor antigens.^{10,11} Immune checkpoint inhibitors (ICIs) are a class of immunotherapeutic agents that work by removing the inhibitory brakes on T cells, resulting in productive antitumor immune responses. However, only a fraction of patients with cancer respond substantially to checkpoint inhibitor immunotherapy.^{12–14} Therefore, it is important to explore the tumor immune microenvironment (TIME) and the tumor response to immunotherapy to improve the prognosis and optimize the immunotherapeutic benefits.

Alternative splicing (AS) is a fundamental step in messenger RNA (mRNA) maturation that increases the diversity and functional capacity of a gene at the posttranscriptional level through the differential use of exons or portions thereof.^{15–17} In general, there are 7 main patterns of AS events: alternate acceptor site (AA), alternate donor site (AD), alternate promoter (AP), alternate terminator (AT), exon skip (ES), mutually exclusive exons (ME), and retained intron (RI).^{18,19} Several studies have shown that AS plays an important role in tumorigenesis, progression, and response to anticancer drug therapy.^{20,21} Especially in the process of tumorigenesis, AS plays a major regulatory role in the cell cycle, the DNA damage response, and apoptosis.²²

While several studies have clarified the correlation with and clinical significance of AS events in bladder cancer biology,^{23–25}

no single gene or molecular marker can accurately predict disease development. The relationship between AS prognostic signature and the TIME and response to immunotherapy and chemotherapy remains obscure. In this study, we identified prognostic signature that is closely related to immune infiltration and the response to immunotherapy and chemotherapy. This may provide recommendations for the establishment of tailored treatment strategies and treatment objectives.

Methods

Bladder Cancer Dataset Source

The AS event data of the The Cancer Genome Atlas Urothelial Bladder Carcinoma (TCGA-BLCA) cohort were obtained from SpliceSeq (<http://bioinformatics.mdanderson.org/TCGASpliceSeq>).²⁶ Samples were screened when the Percent Spliced-In (PSI) value exceeded 0.75. The transcriptome and clinical information of the patients with bladder cancer were downloaded from The Cancer Genome Atlas (TCGA) database (<https://portal.gdc.cancer.gov/>). The analytical process flowchart is shown in Supplementary Figure S1.

Identification of Survival-Associated AS Events

Samples with clinical follow-up and AS data were included in the study. Cases were excluded if: (1) the overall survival (OS) of patients was 0 days; (2) the standard deviation of the PSI value was < .01. Univariate Cox regression analysis was performed to explore the relationship between the AS event and the OS of patients with bladder cancer. An UpSet plot was used to visualize the associations between genes and each type of AS event. A bubble plot was applied to summarize the top 20 most significant AS events from each subtype.

Construction and Validation of Prognostic Signatures

The least absolute shrinkage and selection operator (LASSO) penalty was employed in each splicing pattern and integrated splicing pattern to build 8 optimal prognostic signatures. Ten-fold cross-validation was applied to tune the optimal value of the penalty parameter. The identified AS events were

introduced into multivariate Cox regression analysis to filter the prognostic predictors. Subsequently, prognostic signatures were built and the formula for computing the risk score is as follows: risk score = β_{AS} event1 × PSIAS event1 + β_{AS} event2 × PSIAS event2 + ... + β_{AS} eventn × PSIAS eventn. The performance of the prognostic signatures was evaluated using Kaplan–Meier survival analysis, the proportional hazards model, and time-dependent receiver operating characteristic (ROC) analysis.

Construction of a Prognostic Nomogram

A prognostic nomogram including the AS-based risk score, age, and the pathologic stage was established to estimate quantitatively the 1-, 2-, and 3-year OS probability. The performance of the nomogram was evaluated using a calibration curve.

Correlation of the Risk Score with Tumor-Infiltrating Immune Cell Characterization

Immune infiltration information consisting of every specimen of the immune cell fraction (ie B cells, CD4+T cells, CD8+T cells, dendritic cells, macrophages, neutrophils, etc.) were downloaded from the tumor immune estimation resource (TIMER) (<https://cistrome.shinyapps.io/timer/>). The correlation between tumor immune cells and the prognostic risk score was determined. The immune and stromal scores were downloaded from the Estimation of Stromal and Immune cells in MAlignant Tumor tissues using Expression data (ESTIMATE) (<https://bioinformatics.mdanderson.org/estimate>). sample gene set enrichment analysis (ssGSEA) via the R package “GSEAbase” was used to evaluate the immune-related characteristics in different risk subgroups. To further explore the immune and risk score, the CIBERSORT algorithms in the R platform were used to calculate the fraction of immune cell types.

Effect of the Risk Score on Prediction of the Response to Immunotherapy and Chemotherapy

We compared the expression levels of immune-checkpoint-block-related genes between low-risk and high-risk groups. The relationship between the AS-related prognostic signature and the response to immunotherapy was predicted using the Tumor Immune Dysfunction and Exclusion (TIDE) web tool (<http://tide.dfci.harvard.edu/>). In addition, we used the “pRRophetic” package in R to predict the sensitivity (half maximal inhibitory concentration [IC50]) of chemotherapeutics in the 2 risk score groups of patients with bladder cancer and to infer the sensitivity of the different patients.

Functional Annotation

ClusterProfiler was applied to explore Gene Ontology (GO) term enrichment and Kyoto Encyclopedia of Genes and Genomes (KEGG) analyses of genes corresponding to the significant survival-associated AS events. A false-discovery rate (FDR) < 0.05 was considered statistically significant.

Construction of the Correlation Network of Survival-Associated AS Events and SFs

A catalogue of 404 splicing factors (SFs) was obtained from a previous study.²⁷ The expression profiles of these SFs were downloaded from the TCGA database. The association between the SFs and the survival-relevant AS events was evaluated using Spearman’s correlation analysis. Finally, the underlying SFs-AS regulatory network was built using Cytoscape (version 3.9.0).

Statistical Analyses

The Wilcoxon test was employed to compare 2 groups, whereas the Kruskal–Wallis test was carried out to compare more than 2 groups. Pearson’s correlation coefficient was used to evaluate the correlation between 2 continuous variables. The hazard ratio (HR) and 95% confidence interval (CI) were calculated using a Cox regression model of the survival package, and the Kaplan–Meier method was used for survival analysis. The R package “Hmisc” was used to calculate the C-index of the nomogram. The closer the C-index is to 1, the better the discriminant ability of the nomogram. All statistical tests were performed with R statistical software (v4.1.1).

Results

Clinical Characteristics and Integrated AS Event Data in Bladder Cancer

The TCGA database includes 413 patients with bladder cancer, of which 388 patients were included and 25 patients were excluded because of incomplete information. The basic clinical characteristics of the patients are shown in Table 1.

Table 1. Baseline data of all bladder cancer patients

Characteristic	Type	n	Proportion (%)
Age	<=65	142	36.60
	>65	246	63.40
Gender	Female	102	26.29
	Male	286	73.71
Grade	High	374	96.39
	Low	12	3.09
	Unknown	2	0.52
Stage	Stages I to II	119	30.67
	Stages III to IV	268	69.07
	Unknown	1	0.26
T stage	T1-2	187	48.2
	T3-4	195	50.26
	Unknown	6	1.55
M stage	M0	183	47.16
	M1	11	2.84
	Unknown	194	50
N stage	N0-1	267	68.81
	N2-3	81	20.88
	Unknown	40	10.31

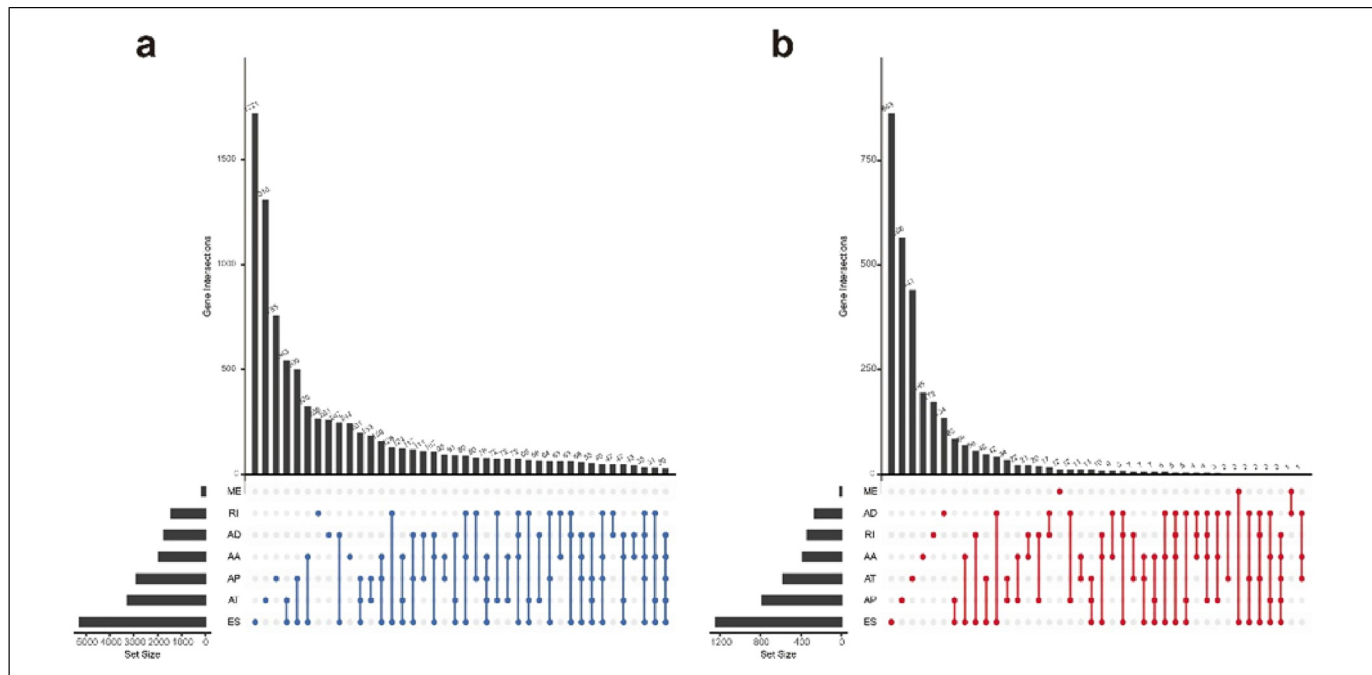


Figure 1. UpSet plots of alternative splicing (AS) events in bladder cancer. The horizontal axis represents the number of genes in each AS type. The vertical axis represents the number of genes for one or several splicing types. (a) The gene interactions among the 7 types of AS events in The Cancer Genome Atlas Urothelial Bladder Carcinoma (TCGA-BLCA) cohort. (b) The gene interactions among the 7 types of survival relevant AS events.

Survival-Associated AS Events in the Bladder Cancer Cohort

The gene intersections among the 7 subtypes of AS events are presented in an UpSet plot (Figure 1a). ES is the most common splicing pattern, followed by AT and AP. To investigate the effect of AS events on bladder cancer survival, 4684 AS events significantly associated with survival were confirmed by univariate Cox regression analysis (Supplementary Table S1). Most AS events were correlated with prognosis, and one gene might have many survival-associated AS events in patients with bladder cancer. The gene intersections among the 7 subtypes of AS events significantly associated with survival are presented in an UpSet plot (Figure 1b). ES is the most common splicing pattern, followed by AP and AT. The volcano map shows all AS events (Figure 2a) and the bubble chart shows the top 20 survival-related AS events among integrated and individual AS patterns (Figure 2b-i).

Prognostic Predictors for Patients with Bladder Cancer and Correlation of Prognostic Signatures with Clinical Features

The LASSO penalty and multivariate Cox regression analysis were used to evaluate the prognostic performance of the top significant survival-related AS events (Figure 3a-b, Supplementary Figure S2a-g and S3ag, Supplementary Table S2). A final prognostic risk model of bladder cancer was established based on 10 genes (eg APOEBC3D, SPINK1, TBC1D3F, LCOR, DZIP1, WDR18, DDX11, CLU, LMF2, and PSTK). Based on the

cut-off value of the median risk score, the samples were divided into a high-risk group and a low-risk group. Heatmaps display the distributions of AS event PSI values for the low- and high-risk groups (Figure 3c, Supplementary Figure S4a, S4d, S5a, S5d, S6a, S6d, and S7a). The allocations of the risk score (Figure 3d, Supplementary Figure S4b, S4e, S5b, S5e, S6b, S6e, and S7b) and dot plots of the survival status (Figure 3e, Supplementary Figure S4c, S4f, S5c, S5f, S6c, S6f, and S7c) suggest that high-risk patients with bladder cancer have a shorter OS. Kaplan-Meier survival analysis showed that the OS of the high-risk group is worse than that of the low-risk group ($P<.05$) (Figure 3f, Supplementary Figure S8a, S8c, S8e, S8g, S9a, S9c, and S9e). ROC analysis (Figure 3g, Supplementary Figure S8b, S8d, S8f, S8h, S9b, S9d, and S9f) indicated that the prognostic signatures of bladder cancer present a good predictive ability. COX regression analysis showed that the pathologic stage, age, and risk score are independent prognostic factors of bladder cancer (Figure 3h and i and Supplementary Figure S10a-n).

Construction of an AS-Clinicopathological Nomogram

Based on the above independent prognostic factors, including the risk score, the pathologic stage, and age, a nomogram was constructed to predict bladder cancer survival at 1, 2, and 3 years (Figure 4a). The patient's pathologic stage, age, and risk score were assigned according to the top points. Verification of the nomogram produced a C-index of 0.823 (95% CI: 0.741-0.905), suggesting that the nomogram has a good degree of differentiation. The calibration curve

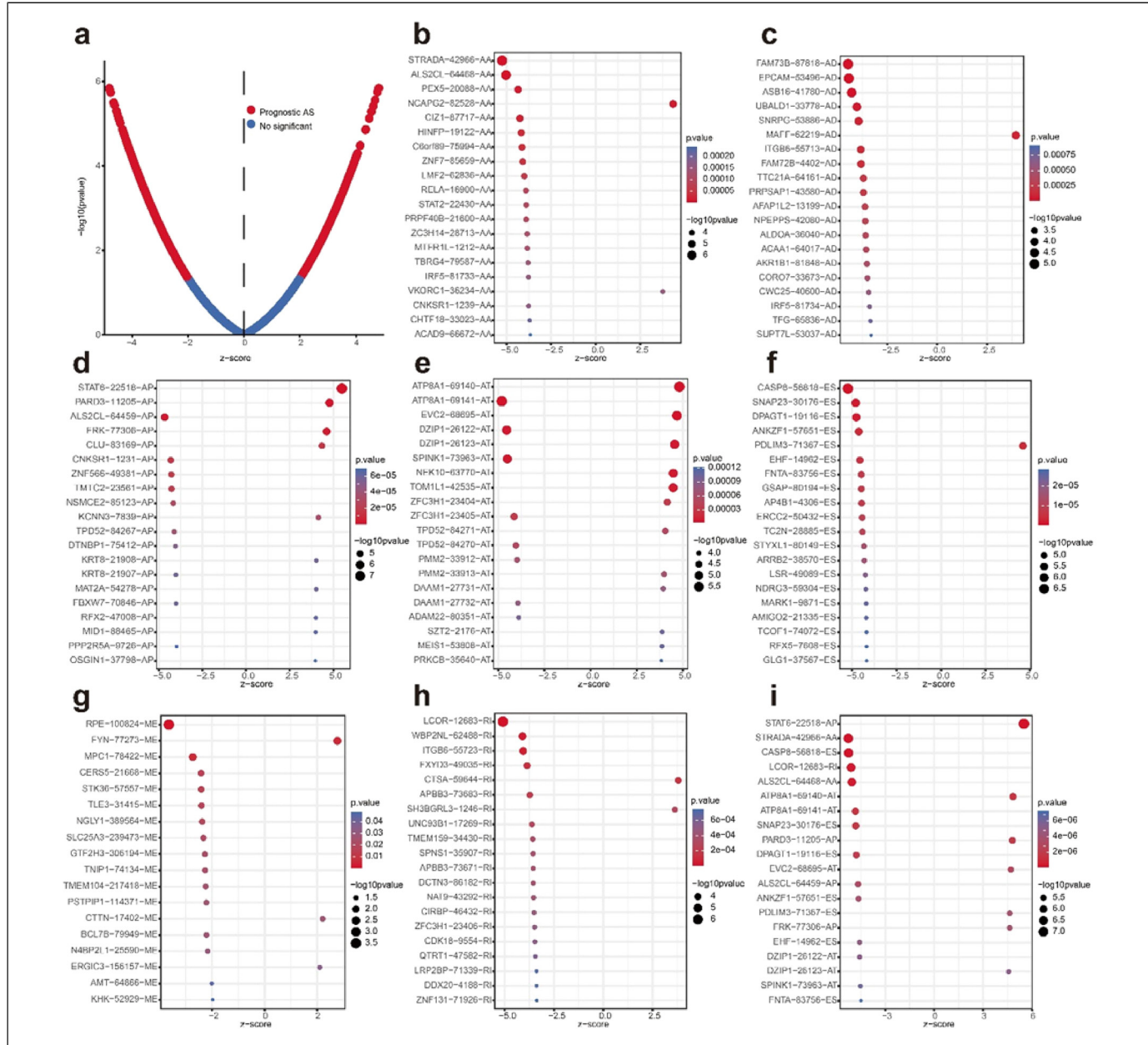


Figure 2. The survival-relevant alternative splicing (AS) events. (a) The blue dots represent insignificant AS events, whereas the red dots represent prognosis-related AS events. The most significant survival-relevant AA, AD, AP, AT, ES, ME, and RI in The Cancer Genome Atlas Urothelial Bladder Carcinoma (TCGA-BLCA) cohort (b-i). The vertical axis represents the ID of the specific AS event. Events with greater significance are represented by larger circles and are colored in red.

Abbreviations: AA: alternate acceptor site; AD: alternate donor site; AP: alternate promoter; AT: alternate terminator; ES: exon skip; ME: mutually exclusive exons; RI: retained intron

(Figure 4b-d) showed good consistency between the predicted and observed values for 1-, 2-, and 3-year survival, suggesting that the nomogram has good predictive power.

Correlation of Risk Scores with the TIME

To further explore the role of the prognostic risk score in immunity, we used TIMER and found that the prognostic signature is positively associated with CD8+ T cells ($r = 0.25, P = 9.4E-07$), dendritic cells ($r = 0.20, P = 1E-04$),

macrophages ($r = 0.17, P = 0.00062$), and neutrophils ($r = 0.14, P = 0.0074$), suggesting greater immune cell infiltration in the high-risk group (Figure 5a-d and Supplementary Figure S11a-b). Similarly, the ESTIMATE results (Figure 5e-g) suggest a higher immune score, stroma score, and ESTIMATE score in the high-risk group. We also elucidate the enrichment of 29 immune-function-related gene sets (Figure 5h-i) in the 2subgroups using ssGSEA. “Neutrophil”, “Macrophage”, “Regulatory.T.cell”, “T.follicular.helper.cell”, “Activated.dendritic.cell”,

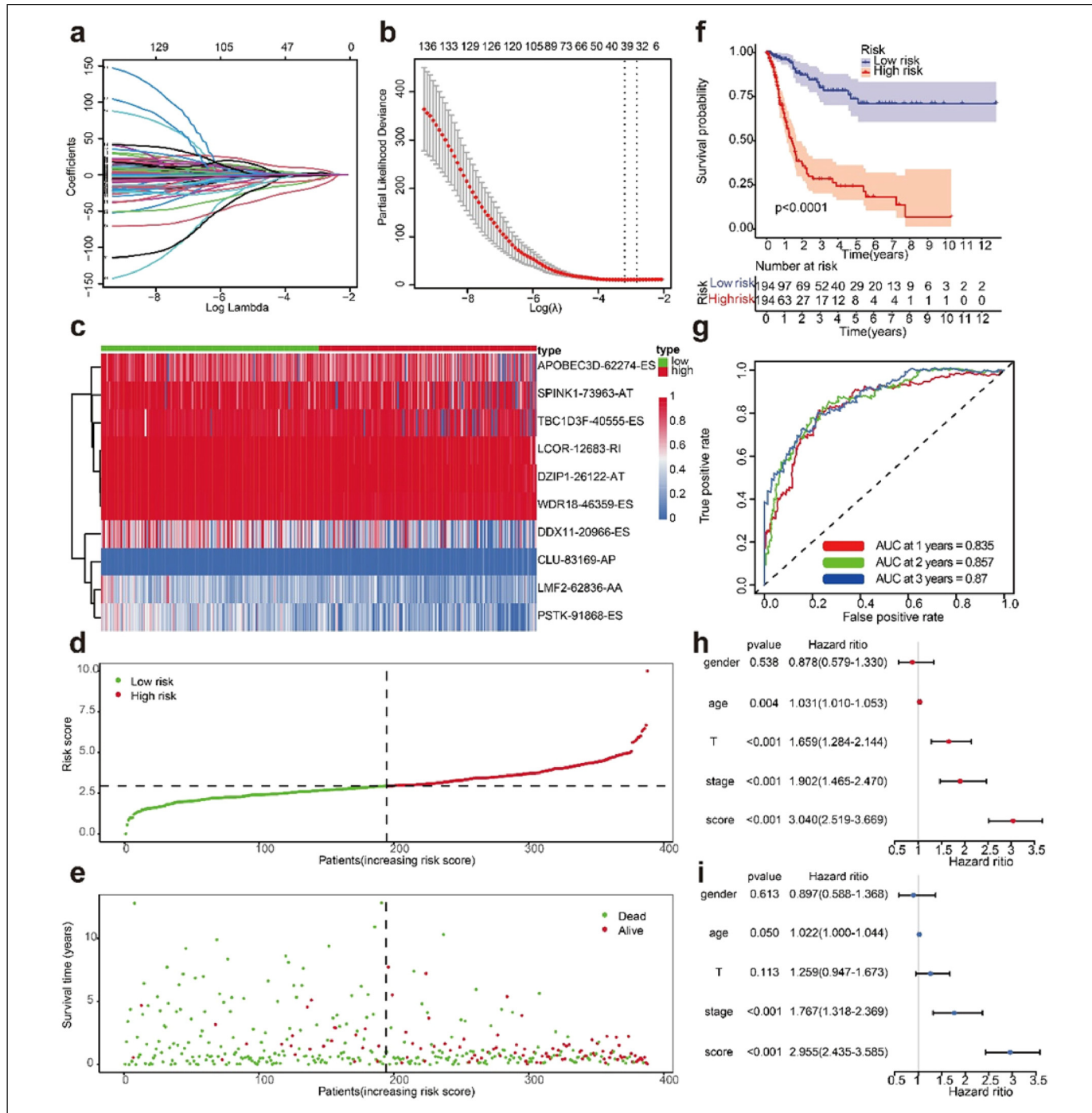


Figure 3. Identification of the integrated alternative splicing (AS)-based prognostic signature. (a) LASSO coefficient profiles of the whole AS events. The horizontal axis represents the Log Lambda. The vertical axis represents the coefficients. (b) Ten-fold cross-validation for tuning parameter selection in the lasso regression. The lowest point of the ordinate is the minimum point of the cross-validation error. (c) Heatmap of PSI values of AS events for building the final prognostic signature. (d) Distribution of the signature risk score. (e) The survival status and survival duration of patients with bladder cancer. (f) Kaplan–Meier plot presenting survival in the high-risk and low-risk groups. (g) Received operating characteristic (ROC) analysis for the final prognostic signature based on all 7 types of AS events. (h) Univariate Cox regression results. (i) Multivariate Cox regression results.

Abbreviations: LASSO: least absolute shrinkage and selection operator; PSI: Percent Spliced-In.

“Plasmacytoid.dendritic.cell”, and “Central.memory.cd8.T.cell” increase as the risk score increases. The CIBERSORT algorithm results (Figure 5j) showed the fraction of 22 immune cell types

in 2 subtypes. We can find that “NK cells resting” and “B cells memory” have a higher proportion in the low-risk groups. These results suggest that the prognostic signature may be a method to

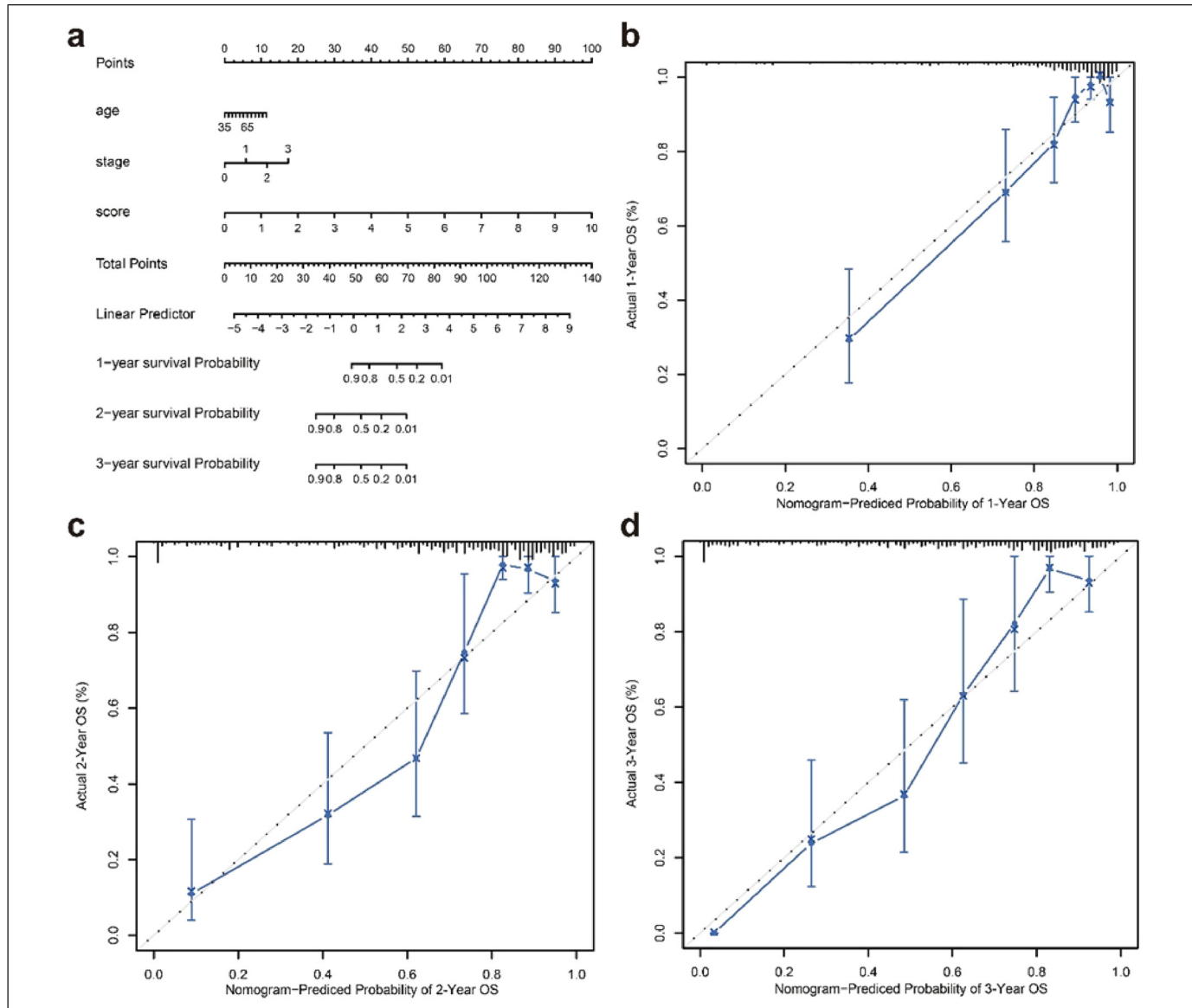


Figure 4. Identification of the composite prognostic nomogram. (a) Composite nomogram prediction of 1-, 2-, and 3-year overall survival (OS). (b) One-year nomogram calibration curves. (c) Two-year nomogram calibration curves. (d) Three-year nomogram calibration curves.

identify immune characteristics and predict the immune microenvironment of bladder cancer.

Correlation of Integrated Signature with ICIs Key Molecules and the Response to Chemotherapy

Given the differences in the immune microenvironment between low-risk and high-risk groups, we investigated the relationship between the prognostic signature and drug responses to encourage individualized treatment decisions. We found significant differences in the expression of 46 immune-checkpoint-related genes between the low-risk and high-risk groups (Figure 6a). We also compared TIDE scores (Figure 6b) in the low-risk and high-risk groups; they are higher in the high-risk group, suggesting that the low-risk group may

benefit from ICIs, while the high-risk group has a greater chance of immune escape. In addition, we analyzed the relationship between the prognostic signature and responses to several common chemotherapeutic agents (Figure 6c-e), revealing that patients with a low-risk score are more sensitive to methotrexate, while patients with a high-risk score are more sensitive to cisplatin and docetaxel. These results suggest the prognostic signature might be used as an indicator for treatment selection.

Functional Enrichment Analysis

We investigated the specific biological functions of these prognosis-related AS events using KEGG and GO functional enrichment analyses. The results (Figure 7a-b) indicated the top 8 terms of functional enrichment analyses, such as RNA

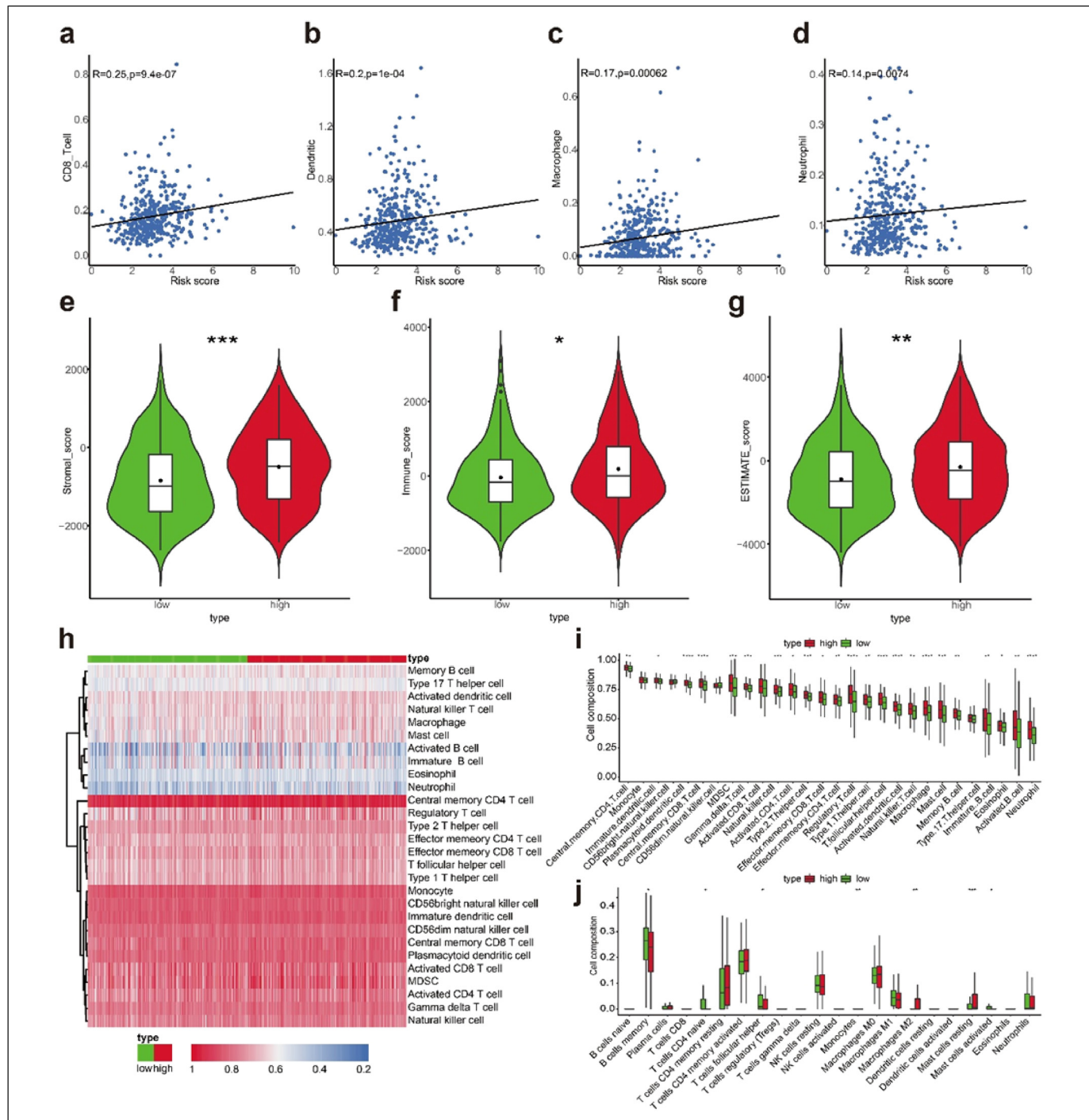


Figure 5. Relationship between infiltrating immune cells and the final alternative splicing (AS) prognostic signature. (a) Correlation between this signature and CD8 + T cells. (b) Correlation between this signature and dendritic cells. (c) Correlation between this signature and macrophages. (d) Correlation between this signature and neutrophils. (e) Violin plot for the stromal score between the low-risk and high-risk groups. (f) Violin plot for the immune score between the low-risk and high-risk groups. (g) Violin plot for the ESTIMATE score between the low-risk and high-risk groups. (h) Heatmap of enrichment of 29 immune signatures for the final prognostic signature. (i) Distinction of enrichment of immune-related signatures for the low-risk and high-risk groups. (j) Difference of infiltrating immune cell subpopulations and levels for the low-risk and high-risk groups.

Abbreviation: ESTIMATE: Estimation of Stromal and Immune cells in MAlignant Tumor tissues using Expression data.

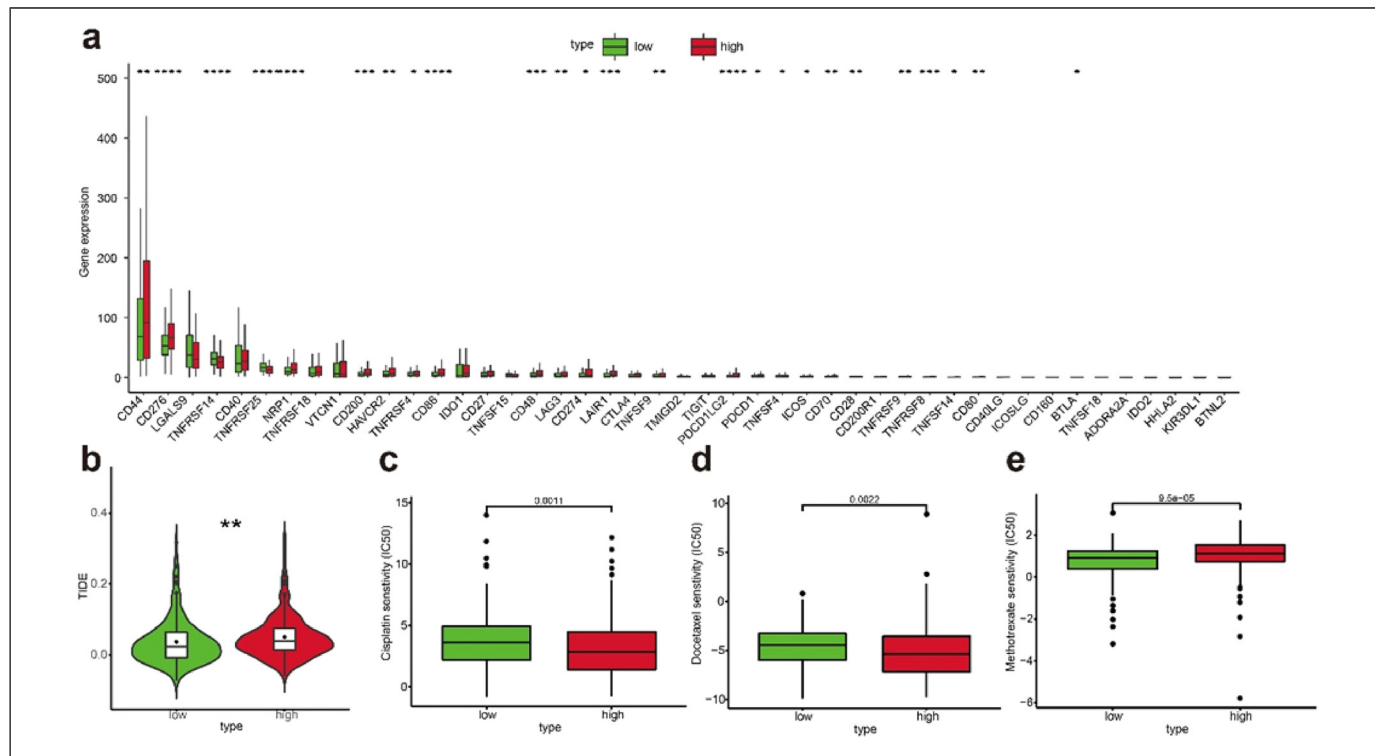


Figure 6. Immune checkpoint and prediction of the response to immunotherapy and chemotherapy. (a) Comparison of immune checkpoint blockade-related genes expression levels between the low-risk and high-risk groups. (b) Violin plots of TIDE scores for patients with bladder cancer in the high-risk and low-risk groups. (c) Sensitivity analysis of patients taking cisplatin at high and low risk. (d) Sensitivity analysis of patients taking docetaxel at high and low risk. (e) Sensitivity analysis of patients taking methotrexate at high and low risk.

Abbreviation: TIDE: Tumor Immune Dysfunction and Exclusion.

splicing, nuclear envelope, transcription coregulator activity, and ubiquitin-mediated proteolysis.

Correlation Between Survival-Associated AS Events and SFs Expression

We constructed the potential regulatory network among the significant survival-related AS events and SFs (Figure 8). It comprises 276 pairs of correlations that involve 23 SFs and 119 AS events (Supplementary Table S3). In addition, the expression of most SFs is positively correlated with adverse AS events but negatively correlated with favorable AS events. Among these factors, EIF3A, DDX21, SDE2, TNPO1, and RNF40 control many AS events, suggesting that they may play an important role in bladder cancer.

Discussion

Bladder cancer is the most common urological malignancy worldwide. Immunotherapy has achieved good results in bladder cancer, but how to better understand the heterogeneity of bladder cancer remains the key issue.²⁸ AS serves as an important mechanism for cell development, differentiation, and regulation of cell functions. The process has been involved in various diseases, including cancers. For example, Daniel J Coleman et al reveal the role of SRRM4-mediated AS of LSD1 + 8a in neuroendocrine prostate

cancer.²⁹ Ruihui Xie et al found that RBMX reduces bladder cancer tumorigenicity and progression via a hnRNP A1-mediated PKM AS mechanism.³⁰ Therefore, AS-related biomarkers are potential diagnostic biomarkers and therapeutic targets in patients with bladder cancer. Previous studies have studied the role of AS or immunotherapy in bladder cancer, but ignored the relationship between them. In this study, we constructed a prognostic signature and analyzed the correlation between AS events and the TIME and immunotherapy effects in bladder cancer using bioinformatics and statistical tools.

In this study, we identified 4684 AS events associated with survival and established prognostic signatures. We constructed a comprehensive prognostic nomogram to facilitate clinical practice. Then, we identified prognostic signature that is closely related to immune infiltration and the response to immunotherapy and chemotherapy. In addition, GO term enrichment and KEGG analysis of genes associated with significant survival-related AS events showed that ubiquitin-mediated proteolysis is associated most significantly with survival-related AS events. Finally, we established the SFs-AS regulatory network, revealing that key SFs such as EIF3A, DDX21, SDE2, TNPO1, and RNF40 might regulate AS in bladder cancer.

We downloaded AS data from TCGA SpliceSeq to comprehensively analyze the prognostic value of AS events in patients with bladder cancer. Using univariate Cox regression analysis, we identified 4684 AS events significantly associated with survival and then investigated the prognostic value of these events.

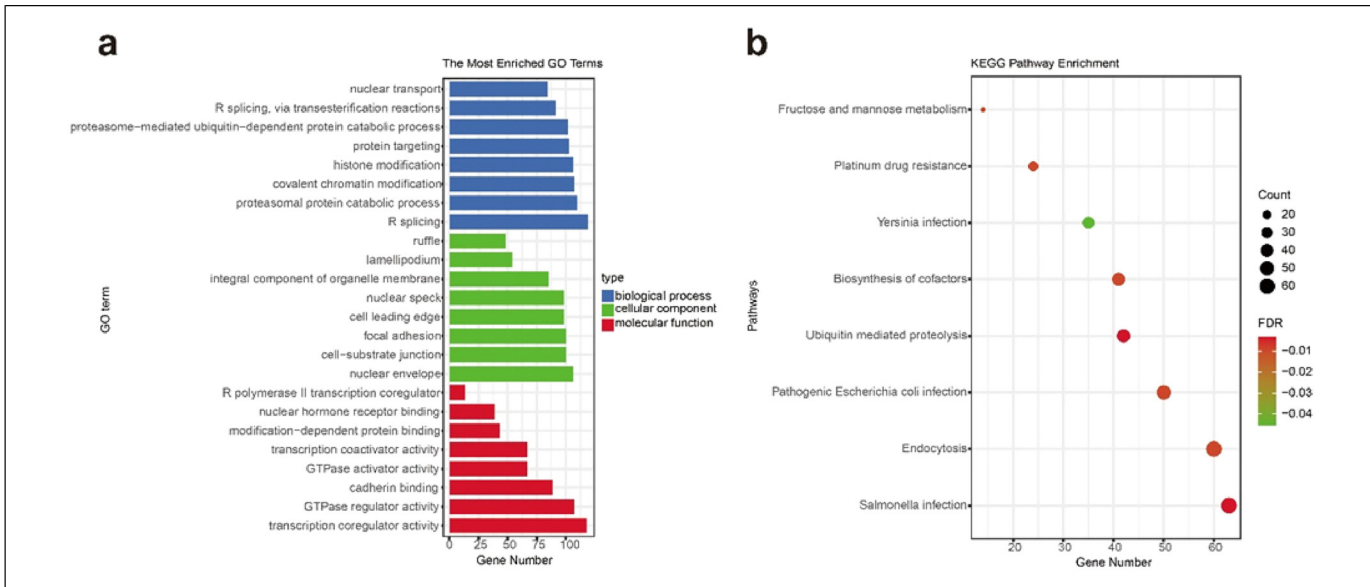


Figure 7. Biological function analysis. (a) Terms identified by Gene Ontology (GO) analysis. (b) Enrichment pathways identified by the Kyoto Encyclopedia of Genes and Genomes (KEGG).

The incidence of ES events was the highest in patients with bladder cancer, suggesting that ES events may have a greater impact on the prognosis of bladder cancer. Subsequently, we proposed final prognostic signatures for bladder cancers. The 8 prediction signatures based on AS patterns all show potential value for the prognosis of patients with bladder cancer. The ROC curve, Kaplan–Meier survival analysis, and multivariate COX regression suggest that the final prognostic signatures could be used as an independent risk factor, indicating that the signatures can more accurately predict the prognosis of bladder cancer. To translate the final risk signature into further clinical practice, we established a composite nomogram by integrating the pathologic stage; the predicted results are in high agreement with the actual results.

To explore the relationship between AS events and the bladder cancer microenvironment and response to immunotherapy, we used a variety of algorithms to assess the TIME and the expression of genes associated with immune checkpoints in bladder cancer. We found that inhibitory immune cells such as regulatory T cells (Tregs), macrophages, and myeloid-derived suppressor cell (MDSC) in the high-risk group have a higher degree of infiltration, and these inhibitory immune cells could promote tumor tissue angiogenesis and tumor cell proliferation, invasion, and metastasis by secreting inflammatory cytokines.^{31,32} Studies have shown that tumor-associated macrophages (TAM) and tumor cells can recruit Tregs to tumor sites by secreting CCL20 or CCL22 and foster immune privilege.³³ The high-risk group has a higher TIDE prediction score, suggesting that it is more prone to immune escape and would not benefit from ICIs therapy.³⁴ This finding implies that the risk score might contribute to developing a tailored immunotherapy.

Further functional enrichment analysis showed that the ubiquitin-mediated proteolysis pathway is correlated most significantly with genes corresponding to these survival-associated

AS events. Ubiquitin is a small, evolutionarily conserved eukaryotic protein.³⁵ Ubiquitin-mediated proteolysis comprises 2 steps: the binding of ubiquitin molecules to protein substrates and the degradation of the polyubiquitin proteins by the 26S proteasome complex, which plays an important role in protein degradation, regulation of the cell cycle, modulation of the immune and inflammatory responses, control of signal transduction pathways, development, and differentiation.^{36–38} Furthermore, many studies have shown that suppressing the ubiquitin-mediated proteolysis pathway promotes the proliferation and migration of tumor cells.^{39–41} Thus, AS events in patients with bladder cancer might impact a variety of biological functions via the ubiquitin-mediated proteolysis pathway.

AS mainly involve SFs interacting with RNA-binding proteins at regulatory sites known as silencers or enhancers.⁴² SFs promote or inhibit splicing events by recognizing splicing regulatory sites on precursor RNA and recruiting and assembling spliceosomes.⁴³ SFs have become a new class of oncoproteins. The abnormal expression of SFs leads to the formation of different mRNA subtypes that are involved in tumor proliferation, migration, and apoptosis.⁴⁴ In this study, we found that 23 SFs are significantly associated with 79 survival-associated AS events in bladder cancer. The network in our analysis indicates that EIF3A, DDX21, SDE2, TNPO1, and RNF40 control a large portion of AS events and adversely affect the prognosis of patients. Previous research has indicated the role of these SFs in the development, progression, and prognosis of multiple tumors.^{45–49} For example, EIF3A plays a pivotal role in the phenotype and prognosis of bladder cancer by affecting the transcriptome.⁴⁹ However, the roles of several other SFs in bladder cancer have not been discussed in previous studies. Therefore, in-depth exploration of the role of these SFs in bladder cancer might help researchers to further explore the

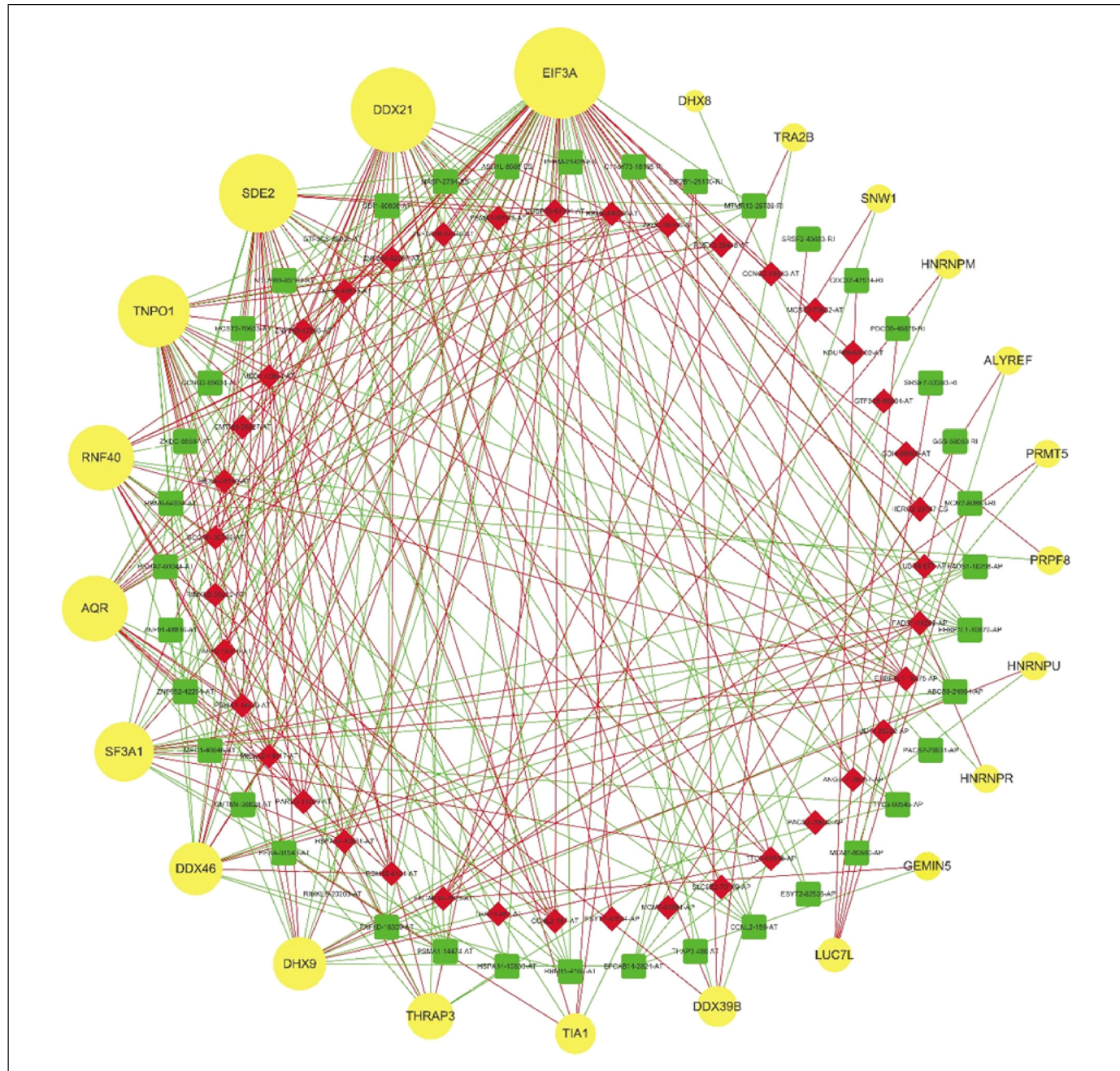


Figure 8. Correlation network between splicing factors (SFs) and survival-related alternative splicing (AS) events generated using Cytoscape. The yellow round bubbles represent SFs, SFs with greater significance are represented by larger circles. Red/green quadrate represents adverse/favorable AS events. Red/green lines represent positive/negative correlations ($r > 0.6$ or $r < -0.6$) between substances.

tumorigenesis of bladder cancer, find new therapeutic targets, and improve the prognosis of patients.

In summary, our study emphasized the prognostic value of AS in bladder cancer, revealed the relationship between AS and the immune microenvironment and immunotherapy. Our findings provided a basis for understanding the role of AS, and indicated the potential clinical significance of AS in the immunotherapy of bladder cancer. However, the current study still has some limitations. Our findings need to be further validated in other independent cohorts to determine the robustness

of the AS prognostic signature. In addition, the relationship between AS and the TIME and immunotherapy effects in bladder cancer still needs a large number of experiments in cell and molecular biology.

Conclusions

Our results highlight a link between AS and bladder cancer prognosis. We established prognostic signatures and an AS-clinico-pathological nomogram to quantitatively predict

the outcome. Besides, functional enrichment analysis and the SFs-AS regulatory network suggest promising targets of the antitumor therapy in bladder cancer. The comprehensive bioinformatic analysis of AS events has robustly linked the AS atlas with the TIME and the response to immunotherapy and chemotherapy in bladder cancer.

Acknowledgments

The authors would like to give our sincere appreciation to the reviewers for their helpful comments on this article and research groups for the TCGA, which provided data for this collection.

Declaration of Conflicting Interests

The author(s) declared no potential conflicts of interest with respect to the research, authorship, and/or publication of this article.

Funding

The study was supported by grants from the Health Commission's Scientific Research Program of Hunan Province (202204074707) to Zhihong Xiao and the Health and Family Planning Commission of Wuhan Municipality (WX18C29) to Zhihong Xiao.

Ethics Statement

Not applicable.

ORCID IDs

Jiang Chen  <https://orcid.org/0000-0002-0826-5244>
 Yangjie Liao  <https://orcid.org/0000-0001-9839-9352>
 Mingjiang Luo  <https://orcid.org/0000-0002-0693-8695>
 Ruirong Tan  <https://orcid.org/0000-0002-4107-2508>

Supplemental Material

Supplemental material for this article is available online.

References

1. Akushevich I, Yashkin AP, Inman BA, Sloan F. Partitioning of time trends in prevalence and mortality of bladder cancer in the United States. *Ann Epidemiol.* 2020;47:25-29. doi:10.1016/j.annepidem.2020.05.006
2. Lenis AT, Lec PM, Chamie K, Mshs MD. Bladder cancer: a review. *JAMA.* 2020;324(19):1980-1991. doi:10.1001/jama.2020.17598
3. Yang J, Li C, Tang Y, et al. Diagnostic roles of proliferative markers in pathological grade of T1 urothelial bladder cancer. *J Cancer.* 2021;12(9):2498-2506. doi:10.7150/jca.52336
4. Kim J, Kim WT, Kim W-J. Advances in urinary biomarker discovery in urological research. *Investig Clin Urol.* 2020;61(Suppl 1):S8-S22. doi:10.4111/icu.2020.61.S1.S8
5. Sun Z, Jing C, Xiao C, Li T. An autophagy-related long non-coding RNA prognostic signature accurately predicts survival outcomes in bladder urothelial carcinoma patients. *Aging (Albany NY).* 2020;12(15):15624-15637. doi:10.18632/aging.103718
6. Mollica V, Rizzo A, Montironi R, et al. Current strategies and novel therapeutic approaches for metastatic urothelial carcinoma. *Cancers (Basel).* 2020;12(6):1449. doi:10.3390/cancers12061449
7. Hinshaw DC, Shevde LA. The tumor microenvironment innately modulates cancer progression. *Cancer Res.* 2019;79(18):4557-4566. doi:10.1158/0008-5472.CAN-18-3962
8. Lei X, Lei Y, Li J-K, et al. Immune cells within the tumor microenvironment: biological functions and roles in cancer immunotherapy. *Cancer Lett.* 2020;470:126-133. doi:10.1016/j.canlet.2019.11.009
9. Chen D, Zhang X, Li Z, Zhu B. Metabolic regulatory crosstalk between tumor microenvironment and tumor-associated macrophages. *Theranostics.* 2021;11(3):1016-1030. doi:10.7150/thno.51777
10. Suresh K, Naidoo J, Lin CT, Danoff S. Immune checkpoint immunotherapy for non-small cell lung cancer: benefits and pulmonary toxicities. *Chest.* 2018;154(6):1416-1423. doi:10.1016/j.chest.2018.08.1048
11. Li B, Chan HL, Chen P. Immune checkpoint inhibitors: basics and challenges. *Curr Med Chem.* 2019;26(17):3009-3025. doi:10.2174/0929867324666170804143706
12. Galani IE, Klechovsky E, Andreakos E. Human and translational immunology in the third millennium: progress, challenges and opportunities. *Nat Immunol.* 2019;20(12):1568-1573. doi:10.1038/s41590-019-0543-6
13. Cao Y, Wang X, Jin T, et al. Immune checkpoint molecules in natural killer cells as potential targets for cancer immunotherapy. *Signal Transduct Target Ther.* 2020;5(1):250. doi:10.1038/s41392-020-00348-8
14. Rizzo A, Mollica V, Massari F. Expression of programmed cell death ligand 1 as a predictive biomarker in metastatic urothelial carcinoma patients treated with first-line immune checkpoint inhibitors versus chemotherapy: a systematic review and meta-analysis. *Eur Urol Focus.* 2022;8(1):152-159. doi:10.1016/j.euf.2021.01.003
15. Cherry S, Lynch KW. Alternative splicing and cancer: insights, opportunities, and challenges from an expanding view of the transcriptome. *Genes Dev.* 2020;34(15-16):1005-1016. doi:10.1101/gad.338962.120
16. Zhao S. Alternative splicing, RNA-seq and drug discovery. *Drug Discov Today.* 2019;24(6):1258-1267. doi:10.1016/j.drudis.2019.03.030
17. Coomer AO, Black F, Greystoke A, Munkley J, Elliott DJ. Alternative splicing in lung cancer. *Biochim Biophys Acta Gene Regul Mech.* 2019;1862(11-12):194388. doi:10.1016/j.bbagr.2019.05.006
18. Chen Q-F, Li W, Wu P, Shen L, Huang Z-L. Alternative splicing events are prognostic in hepatocellular carcinoma. *Aging (Albany NY).* 2019;11(13):4720-4735. doi:10.18632/aging.102085
19. Zhang S, Hu Z, Lan Y, et al. Prognostic significance of survival-associated alternative splicing events in gastric cancer. *Aging (Albany NY).* 2020;12(21):21923-21941. doi:10.18632/aging.104013
20. Ule J, Blencowe BJ. Alternative splicing regulatory networks: functions, mechanisms, and evolution. *Mol Cell.* 2019;76(2):329-345. doi:10.1016/j.molcel.2019.09.017
21. Bonnal SC, López-Oreja I, Valcárcel J. Roles and mechanisms of alternative splicing in cancer - implications for care. *Nat Rev Clin Oncol.* 2020;17(8):457-474. doi:10.1038/s41571-020-0350-x
22. Sciarillo R, Wojtuszkiewicz A, Assaraf YG, et al. The role of alternative splicing in cancer: from oncogenesis to drug resistance. *Drug Resist Updat.* 2020;53:100728. doi:10.1016/j.drup.2020.100728

23. Guo Z, Zhu H, Xu W, et al. Alternative splicing related genetic variants contribute to bladder cancer risk. *Mol Carcinog.* 2020;59(8):923-929. doi:10.1002/mc.23207
24. Thorsen K, Sørensen KD, Brems-Eskildsen AS, et al. Alternative splicing in colon, bladder, and prostate cancer identified by exon array analysis. *Mol Cell Proteomics.* 2008;7(7):1214-1224. doi:10.1074/mcp.M700590-MCP200
25. Han S, Kim D, Shivakumar M, et al. The effects of alternative splicing on miRNA binding sites in bladder cancer. *PLoS One.* 2018;13(1):e0190708. doi:10.1371/journal.pone.0190708
26. Ryan M, Wong WC, Brown R, et al. TCGASpliceseq a compendium of alternative mRNA splicing in cancer. *Nucleic Acids Res.* 2016;44(D1):D1018-D1022. doi:10.1093/nar/gkv1288
27. Seiler M, Peng S, Agrawal AA, et al. Somatic mutational landscape of splicing factor genes and their functional consequences across 33 cancer types. *Cell Rep.* 2018;23(1):282-296.e4. doi:10.1016/j.celrep.2018.01.088
28. Butt S-U-R, Malik L. Role of immunotherapy in bladder cancer: past, present and future. *Cancer Chemother Pharmacol.* 2018;81-(4):629-645. doi:10.1007/s00280-018-3518-7
29. Coleman DJ, Sampson DA, Sehrawat A, et al. Alternative splicing of LSD1 + 8a in neuroendocrine prostate cancer is mediated by SRRM4. *Neoplasia.* 2020;22(6):253-262. doi:10.1016/j.neo.2020.04.002
30. Yan Q, Zeng P, Zhou X, et al. RBMX Suppresses tumorigenicity and progression of bladder cancer by interacting with the hnRNP A1 protein to regulate PKM alternative splicing. *Oncogene.* 2021;40(15):2635-2650. doi:10.1038/s41388-021-01666-z
31. Gajewski TF, Schreiber H, Fu Y-X. Innate and adaptive immune cells in the tumor microenvironment. *Nat Immunol.* 2013;14-(10):1014-1022. doi:10.1038/ni.2703
32. Steevels TAM, Meygaard L. Immune inhibitory receptors: essential regulators of phagocyte function. *Eur J Immunol.* 2011;41(3):575-587. doi:10.1002/eji.201041179
33. Zhang J, Shi Z, Xu X, Yu Z, Mi J. The influence of microenvironment on tumor immunotherapy. *FEBS J.* 2019;286(21):4160-4175. doi:10.1111/febs.15028
34. Jiang P, Gu S, Pan D, et al. Signatures of T cell dysfunction and exclusion predict cancer immunotherapy response. *Nat Med.* 2018;24(10):1550-1558. doi:10.1038/s41591-018-0136-1
35. Dikic I, Wakatsuki S, Walters KJ. Ubiquitin-binding domains - from structures to functions. *Nat Rev Mol Cell Biol.* 2009;10-(10):659-671. doi:10.1038/nrm2767
36. Choi Y, Kim B, Ham S, et al. Subanesthetic ketamine rapidly alters medial prefrontal miRNAs involved in ubiquitin-mediated proteolysis. *PLoS One.* 2021;16(8):e0256390. doi:10.1371/journal.pone.0256390
37. Song J, Merrill RA, Usachev AY, Strack S. The X-linked intellectual disability gene product and E3 ubiquitin ligase KLHL15 degrades doublecortin proteins to constrain neuronal dendritogenesis. *J Biol Chem.* 2021;296:100082. doi:10.1074/jbc.RA120.016210
38. van den Boomen DJH, Volkmar N, Lehner PJ. Ubiquitin-mediated regulation of sterol homeostasis. *Curr Opin Cell Biol.* 2020;65:103-111. doi:10.1016/j.ceb.2020.04.010
39. Meng L-D, Shi G-D, Ge W-L, et al. Linc01232 promotes the metastasis of pancreatic cancer by suppressing the ubiquitin-mediated degradation of HNRNPA2B1 and activating the A-raf-induced MAPK/ERK signaling pathway. *Cancer Lett.* 2020;494:107-120. doi:10.1016/j.canlet.2020.08.001
40. Sun Y, Miller Jenkins LM, Su YP, Nitiss KC, Nitiss JL, Pommier Y. A conserved SUMO pathway repairs topoisomerase DNA-protein cross-links by engaging ubiquitin-mediated proteasomal degradation. *Sci Adv.* 2020;6(46):eaba6290. doi:10.1126/sciadv.aba6290
41. Dang F, Nie L, Wei W. Ubiquitin signaling in cell cycle control and tumorigenesis. *Cell Death Differ.* 2021;28(2):427-438. doi:10.1038/s41418-020-00648-0
42. Yang J, Lv W, Shao L, et al. Pacbio and Illumina RNA sequencing identify alternative splicing events in response to cold stress in two poplar Species. *Front Plant Sci.* 2021;12:737004. doi:10.3389/fpls.2021.737004
43. Zheng X, Peng Q, Wang L, et al. Serine/arginine-rich splicing factors: the bridge linking alternative splicing and cancer. *Int J Biol Sci.* 2020;16(13):2442-2453. doi:10.7150/ijbs.46751
44. Urbanski LM, Leclair N, Anczuków O. Alternative-splicing defects in cancer: splicing regulators and their downstream targets, guiding the way to novel cancer therapeutics. *Wiley Interdiscip Rev RNA.* 2018;9(4):e1476. doi:10.1002/wrna.1476
45. Tanaka A, Wang JY, Shia J, et al. DEAD-box RNA helicase protein DDX21 as a prognosis marker for early stage colorectal cancer with microsatellite instability. *Sci Rep.* 2020;10(1):22085. doi:10.1038/s41598-020-79049-9
46. Luo A, Gong Y, Kim H, Chen Y. Proteome dynamics analysis identifies functional roles of SDE2 and hypoxia in DNA damage response in prostate cancer cells. *NAR Cancer.* 2020;2(2):zcaa010. doi:10.1093/narcan/zcaa010
47. Yang B, Chen J, Li X, et al. TNPO1-mediated nuclear import of ARID1B promotes tumor growth in ARID1A-deficient gynecologic cancer. *Cancer Lett.* 2021;515:14-27. doi:10.1016/j.canlet.2021.05.016
48. Fu J, Liao L, Balaji KS, Wei C, Kim J, Peng J. Epigenetic modification and a role for the E3 ligase RNF40 in cancer development and metastasis. *Oncogene.* 2021;40(3):465-474. doi:10.1038/s41388-020-01556-w
49. Spilka R, Ernst C, Bergler H, et al. eIF3a is over-expressed in urinary bladder cancer and influences its phenotype independent of translation initiation. *Cell Oncol (Dordr).* 2014;37(4):253-267. doi:10.1007/s13402-014-0181-9